Numerical simulation of the 12 May 1997 interplanetary CME event

D. Odstrcil[1]

Cooperative Institute for Research in Environmental Sciences at University of Colorado and National Oceanic and Atmospheric Administration, Boulder, Colorado, USA

P. Riley

Science Applications International Corporation, San Diego, California, USA

X. P. Zhao

W. W. Hansen Experimental Physics Laboratory, Stanford University, Stanford, California, USA

Received 14 July 2003; revised 30 October 2003; accepted 15 December 2003; published 25 February 2004.

[1] Numerical three-dimensional magnetohydrodynamic models are capable of predicting large-scale solar wind structures at Earth, provided that appropriate time-dependent boundary conditions are specified near the Sun. Since knowledge of such conditions is at present insufficient to directly drive the models, various approximations are used. In this paper, we introduce the main features and approximations of a numerical model where (1) the ambient solar wind is derived from coronal models utilizing photospheric magnetic field observations and (2) transient disturbances are derived from geometrical and kinematic fitting of coronagraph observations of coronal mass ejections (CMEs). We have chosen the well-defined halo-CME event of 12 May 1997 as our initial event because it is characterized by a relatively quiet solar and interplanetary background into which the ejecta was launched. The numerical simulation has enabled us to predict the arrival of the shock and ejecta and provided us with a global picture of transient disturbance interacting with a moderately fast solar wind stream. *INDEX TERMS:* 7513 Solar Physics, Astrophysics, and Astronomy: Coronal mass ejections; 2111 Interplanetary Physics: Ejecta, driver gases, and magnetic clouds; 2164 Interplanetary Physics: Solar wind plasma; 3230 Mathematical Geophysics: Numerical solutions; *KEYWORDS:* coronal mass ejection, interplanetary shock, magnetohydrodynamic model, numerical simulation

Citation: Odstrcil, D., P. Riley, and X. P. Zhao (2004), Numerical simulation of the 12 May 1997 interplanetary CME event, *J. Geophys. Res.*, *109*, A02116, doi:10.1029/2003JA010135.

1. Introduction

[2] Numerical three-dimensional (3-D) magnetohydrodynamic (MHD) models are capable of predicting solar wind parameters at the Earth, provided that appropriate time-dependent conditions are specified near the Sun. Since the knowledge of such conditions is at present insufficient to directly drive the models, various approximations are used. Potential field source-surface models have been utilized to derive ambient solar wind parameters at the inner boundary of heliospheric MHD models [e.g., *Usmanov*, 1993; *Odstrcil et al.*, 1998; *Linker et al.*, 1999; *Riley et al.*, 2001]. Time-dependent pulses have been utilized in attempts to simulate transient disturbances, especially shocks, plasma clouds, and magnetic flux ropes [e.g., *Detman et al.*, 1991; *Groth et al.*, 2000; *Manchester et al.*, 2002; *Vandas et al.*, 2002; *Wu et al.*, 1996].

[3] Recently we have conducted studies of 3-D global interactions occurring when a CME (represented by an over-pressured spherical plasmoid) is launched into a tilted streamer belt [*Odstrcil and Pizzo*, 1999a, 1999b]. The present work builds on these results by attempting to simulate observed heliospheric events. Specifically, ambient solar wind is derived from coronal models utilizing photospheric magnetic field observations and transient disturbances are derived from geometrical and kinematic fitting of coronagraph observations of CMEs.

[4] We have chosen the well-defined halo-CME event of 12 May 1997 as our initial event. It is characterized by relatively quiet solar and interplanetary background into which the ejecta was launched; permitting unambiguous identification and tracking of the CME through interplanetary medium up to the near-Earth environment. Note that our approach is similar to other modeling efforts [e.g., *Dryer et al.*, 2001; *Fry et al.*, 2003]; however, in contrast it is based on interpretation of CME observations instead of interpretation of solar flare and type-II radio burst observations to specify shocks. We launch an ejecta that might act like a piston and

[1] On leave from the Astronomical Institute, Ondřejov, Czech Republic.

0148-0227/04/2003JA010135$09.00

generate interplanetary shocks in favorable circumstances. In this paper, we introduce the main features and approximations of the new model and illustrate its abilities and limitations in simulating real heliospheric disturbances.

2. Ambient Solar Wind

[5] The ambient solar wind parameters in the heliosphere are determined by values at the inner boundary. We use data from the SAIC repository of synoptic maps of magnetic field and velocity at 30 R_S [*Linker et al.*, 1999; *Riley et al.*, 2001] (http://www.imhd.net). These data are based on the results of the 3-D MHD coronal solution that provides the magnetic field topology. The coronal solution itself is determined by the photospheric magnetic field observations from the National Solar Observatory at Kitt Peak (http://nsokp.nso.edu, http://synoptic.nso.edu).

[6] The velocity at the source surface (30 R_S) is determined by assuming that: (a) within coronal holes the flow is fast; (b) at the boundary between open and closed field lines the flow is slow; and (c) over a relatively short distance the flow speed is smoothly raised to match the fast coronal hole flow. The boundary of coronal holes is determined from the 3-D coronal MHD model as a boundary between open and closed magnetic field lines (see *Riley et al.* [2001] for details).

[7] The azimuthal magnetic field (B_φ) is determined by $B_\varphi = -B_r \sin(\theta)\, V_{\rm rot}/V_r$, where $V_{\rm rot}$ is the velocity of the source surface corresponding to the 27.2753-day rotation period of the Sun (this value was chosen for convenient storing of parameters at Earth as function of time). The meridional magnetic field and the meridional and azimuthal flow velocities are assumed to be zero. An assumption of the constant momentum flux is used to derive the mass density, and the temperature is chosen to assure thermal pressure balance on the source surface, the inner heliospheric boundary at 30 R_S.

3. Geometrical and Kinematic Properties of the CMEs

[8] Many CMEs observed near the solar limb maintain their angular widths nearly constant as a function of radial height [*Webb et al.*, 1997] and propagate almost radially beyond the first few solar radii [*Plunkett et al.*, 1997]. On the basis of these properties of limb CMEs, the cone model for halo CMEs was developed by *Zhao et al.* [2002] with free parameters that characterize the angular width of the cone and the orientation of the central axis of the cone. The free parameters can be determined by matching the cross section of the cone at a specified radial distance projected on the sky plane with the observed bright ring of the halo CME at a specified time.

[9] The cone model has been applied to reproduce the expanding halo CME observed by LASCO/C3 coronagraph on 12 May 1997 [*Zhao et al.*, 2002]. The best fit suggested an angular width of 50° and a central axis of the cone pointing to N3.0 and W1.0. The CME was determined to be traveling at 650 km/s at 24 R_S (observed at 14:15:05 UT) and was accelerating with about 18.5 m s^{-2}.

[10] Using the above data, we estimate that the leading edge of the CME reached a radial height of 30 R_S at 15:30 UT with a speed of 700 km/s. Further, we estimate that it takes about 8 hours for the CME (with the anticipated diameter of 50°) to pass through that position.

4. Numerical Simulation

[11] The heliospheric model is based upon the ideal 3-D MHD description, with two additional continuity equations used for tracing the injected CME material and the magnetic field polarity (see *Odstrcil and Pizzo* [1999b] for details). The ratio of specific heats, γ, is 1.5. A modified high-resolution TVD Lax-Friedrichs scheme is used [*Toth and Odstrcil*, 1996]. A spherical coordinate system is used where the radius (heliocentric distance, r) is measured from Sun center, meridional angle (co-latitude, θ) is measured down from the north pole (solar rotation axis), and azimuthal angle (longitude, φ) is phased such that the Earth's position is fixed at $\varphi = 180°$. Note that the Earth's position varies in θ due to the 7.25° inclination of the equator to the ecliptic. The computational domain used is a sector spanning 0.14 AU to 1.14 AU in heliocentric distance, 30° to 150° in meridional angle, and 0° to 360° in azimuthal angle. A uniform grid is used, with $\Delta r = 0.0039$ AU, $\Delta\theta = 2°$, and $\Delta\varphi = 2°$. The computational mesh is thus $256 \times 60 \times 180$.

[12] The inner heliospheric boundary conditions of the MHD code are specified as time-dependent values at the source surface at 30 R_S. First, a numerical relaxation is used to establish an ambient state prior to 12 May 1997 by starting computations 150 hours earlier. Then, a time-dependent pulse superimposed on the source surface map is used to introduce the over-pressured plasma cloud (simulating the CME). We use a spatial (circular) shape with a 5°-wide transition zone, and a temporal (trapezoidal) profile with 1-hour ramps as described by *Odstrcil and Pizzo* [1999a]. In this paper, the pulse central axis, diameter, start time, and duration correspond to the fitted values given in the previous section.

[13] The plasma cloud has a uniform velocity corresponding to the fitted CME speed. Further, we have assumed the cloud's density (temperature) to be four times larger than (equal to) the mean values in the fast stream. Thus the plasma cloud has about four times larger pressure than the ambient fast wind. Note that the density values within the cloud are about as large as maximum values in the slow streamer belt at the source surface.

[14] The CME cone model is based on observational evidence that CMEs have more or less constant angular diameter in the corona; i.e., they are confined by the external magnetic field. Thus they do not expand in latitude in the lower corona. However, they can expand in interplanetary space (if they were over-pressured originally) due to the weaker external field. Our model is of course a simplification; however, launching an over-pressured plasma cloud at 30 R_S crudely represents the above scenario.

5. Results and Discussion

[15] Figure 1 shows the distribution of parameters at the heliospheric inner boundary for two different cases; without and with the input pulse. Note that there is a small excursion of the fast stream from the southern coronal hole up to the solar equator at longitude of 180°. Further, note that the

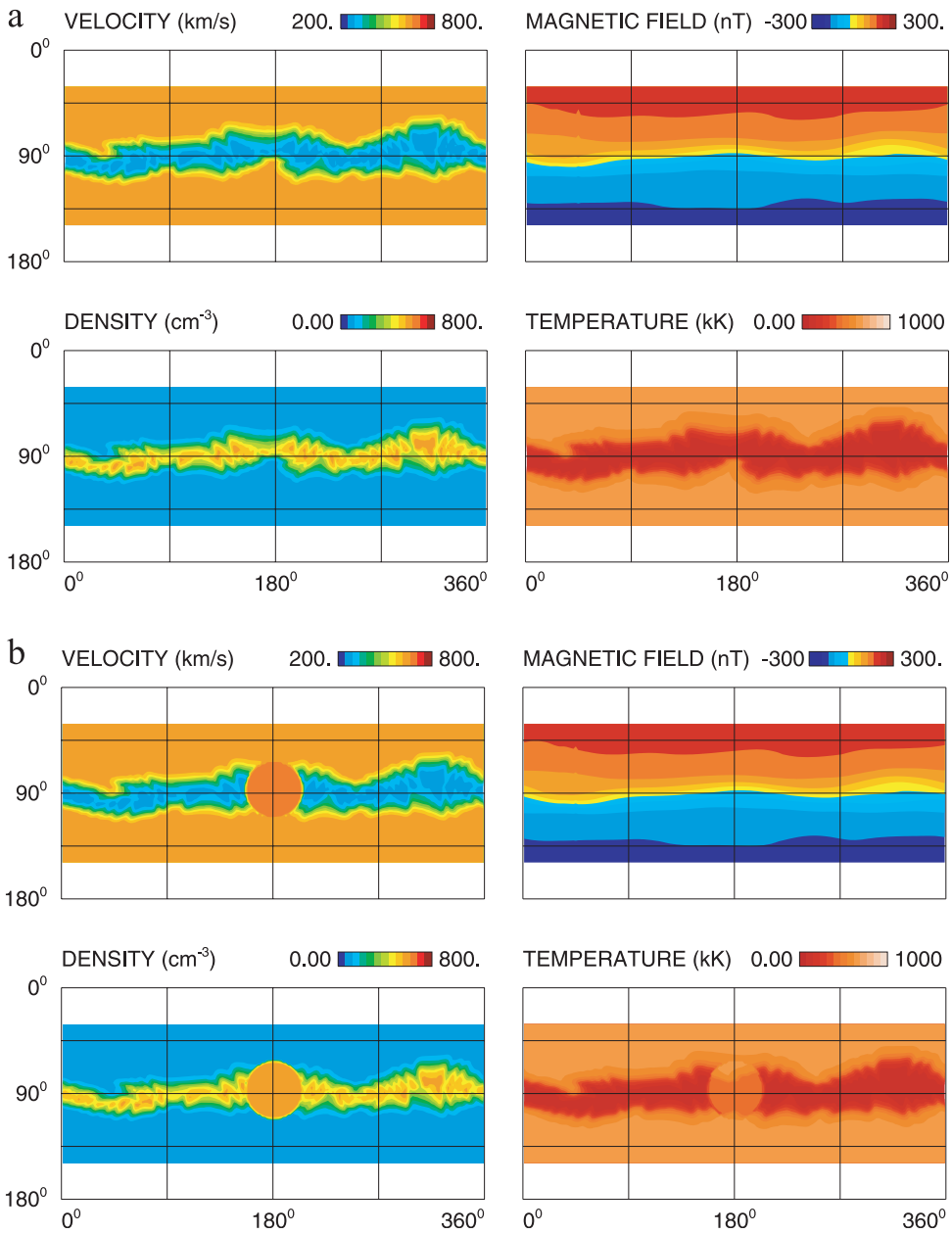

Figure 1. Distribution of solar wind parameters (flow velocity, magnetic field strength, number density, and temperature) on the source surface (the inner heliospheric boundary of the heliospheric model) at 0.14 AU on 12 May 1997 at 15:30 UT, for the case without (top panels) and with (bottom panels) introduction of the transient pulse.

simulated CME is launched into a slow streamer belt in agreement with most observations [*Hundhausen*, 1993; *Zhao and Webb*, 2003]. The inferred central axis location of the 12 May 1997 halo CME (N3.0, W1.0) is in between the solar disk center and the active region 8038 (N23.0, W7.0). *Webb et al.* [2000] observed that the moving part of the erupting filament was directed toward the solar equator and suggested that this filament was probably only a small portion at the base of the much larger mass ejection, which in white light appeared to arise from near disk center.

[16] Figures 2, 3, and 4 show the traveling interplanetary disturbance (at two different times) in the 3-D heliospace. The simulated over-pressured CME acquires much larger angular size than the streamer belt, thus different parts of the ICME propagate in solar wind with different convective velocities. This causes significant latitudinal distortion in the CME shape as can be seen in Figure 2. Note that we consider hydrodynamic ejecta only; thus the distortion is very large. For ICMEs with embedded magnetic structure, tension in the field lines will reduce but not eliminate the distortion [see *Schmidt and Cargill*, 2001].

[17] *Webb et al.* [2000] reported an increasing speed profile across the ICME, which is somewhat unusual at Earth, and they suggested that the ICME was compressed from behind by a high-speed stream. The numerical simulation provides us with a global picture of a transient

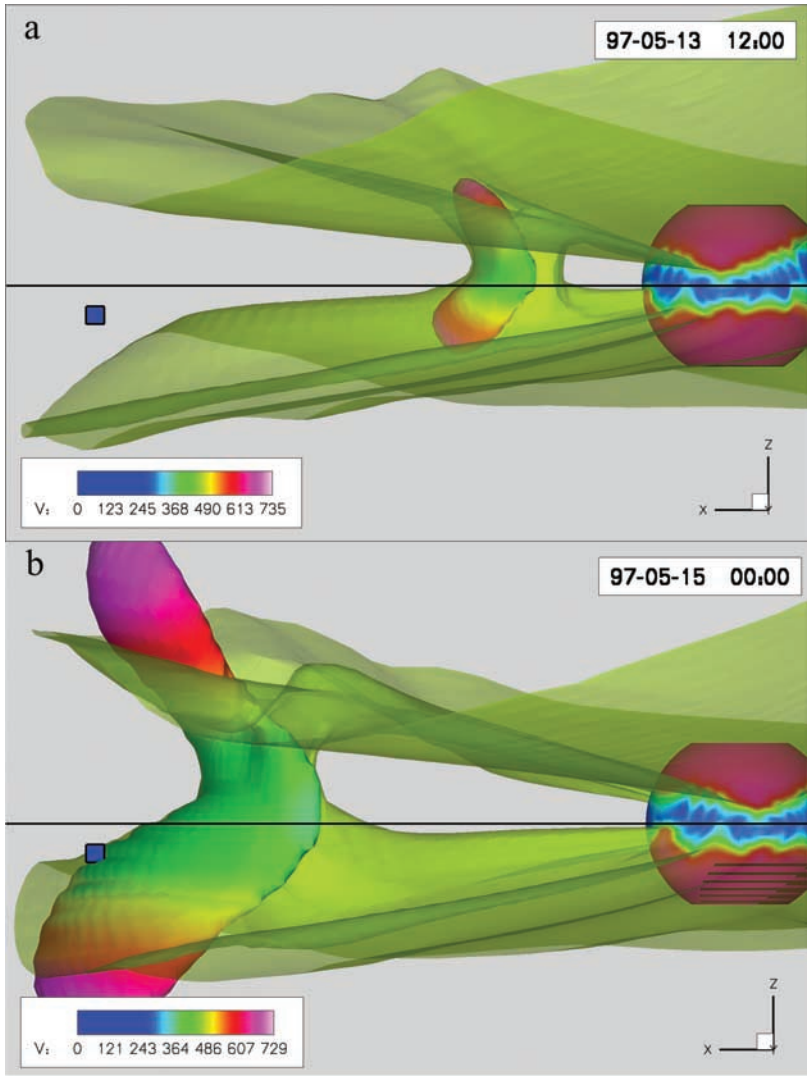

Figure 2. Visualization of disturbed solar wind velocity parameters on May 13 12:00 UT (top panel) and May 15 00:00 UT (bottom panel). Boundaries between the slow streamer belt flow and northern and southern fast wind are shown as translucent iso-surfaces at 475 km s^{-1}. The injected cloud is shown as an iso-surface at 25% of maximum value of its density (scaled by $(R_{AU}/r)^2$); the iso-surface is colored according to the corresponding value of the solar wind velocity. The Earth position is shown by a blue box.

disturbance interacting with background solar wind. The simulated CME propagates on and slightly ahead of the moderate fast stream that results from the excursion of the southern coronal hole toward the helio-equator (Figure 3). The initially fast ICME propagates into the dense slow streamer belt (Figure 4). Faster flow from behind and dense slow plasma ahead favors significant compression of the ejecta in agreement with *Webb et al.* [2000].

[18] The injected CME initially propagates approximately twice as fast as the background ambient flow in the streamer belt and slightly faster than the fast streams. Thus significant interaction occurs only in a latitudinally narrow region where compression waves steepen into a shock. This can be seen in the iso-surfaces of density in Figure 4 where, in addition to dense streamer flows, there is a highly compressed arc at the leading edge of the plasma cloud (note that these structures merge at the westward side). Distortion of magnetic field lines is caused by shock compression and field line draping. Note that for visualization purposes we traced field lines starting from the same position (i.e., they do not corotate) at the equator and 20° above.

[19] Figure 5 shows the evolution of the plasma parameters at Earth (for two different cases: without and with the ICME). According to *Cane and Richardson* [2003], the 12 May 1997 event had the following characteristics at Earth: (1) shock arrived on May 15 at 01:59 UT, (2) ICME started on May 15 at 09:00 UT, and (3) ICME ended on May 16 at 00:00 UT. Our simulations show reasonable agreement with observed flow parameters, as can be seen in Figure 5. However, there is apparently no shock separated from the leading edge of the ICME in our results at Earth. The ambient coronal model produces a fast stream flow with a

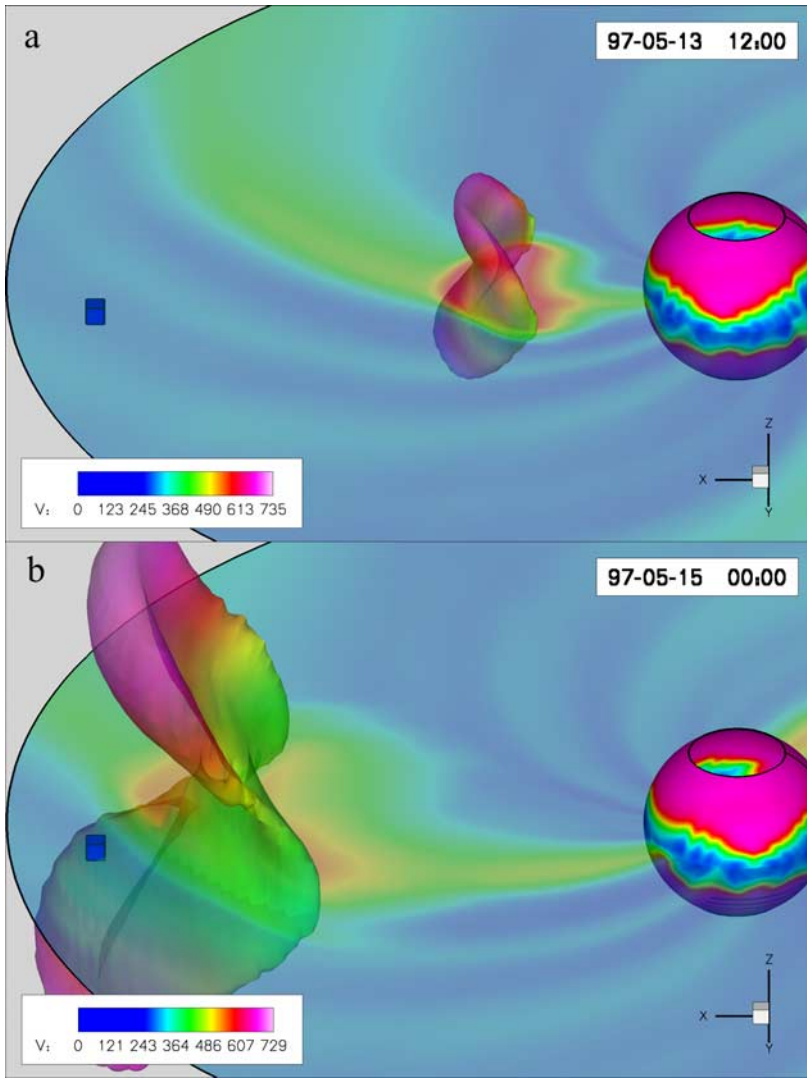

Figure 3. Visualization of disturbed solar wind parameters on May 13 12:00 UT (top panel) and May 15 00:00 UT (bottom panel). The flow velocity is shown on the source surface and on the equatorial plane using the color scale (the coloring on the equatorial plane is translucent). The injected cloud is shown as an iso-surface at 25% of maximum value of its density (scaled by $(R_{AU}/r)^2$; the iso-surface is colored according to the corresponding value of the flow velocity. The Earth position is shown by a blue box.

velocity more than 200 km/s greater than that in the streamer belt flow. The injected cloud has thermal pressure about four times larger than the surrounding fast stream values and a speed about 50 km/s higher initially. This is sufficient to generate a shock within the fast stream. However, later on the disturbance reaches the leading edge of the co-rotating interaction region where the density increases and temperature decreases. This, together with decrease in the flow velocity, causes sudden decrease in characteristic speeds. The cloud-driven pressure waves become attached to the leading edge of the co-rotating fast stream and it is difficult to separate the two. This effect has been observed and discussed earlier [*Odstrcil and Pizzo*, 1999a], wherein it was shown that an interplanetary shock separates from the driving cloud where the initial cloud over-pressure is sufficiently large and/or for a configuration where the cloud is launched ahead of the fast stream.

[20] Numerical simulation of the transient disturbances (bottom panels in Figure 5) is to be compared with numerical simulation of the ambient state (top panels in Figure 5). For example, the large jump in magnetic field is caused by increased draping of interplanetary magnetic field by the ejected cloud (compression by shock/pressure wave is relatively weak at this location), which is superimposed on the previously enhanced (2–3 times) field at the leading edge of the fast stream. This moderate fast stream (a localized excursion of the southern coronal hole) plays an important role in our simulations. It is only about 10–20° wide (see top panels in Figure 1), near the spatial resolution limits of currently available source surface models driven by 27-day averaged synoptic maps, especially when coronal hole boundaries are modified during the eruption process. We plan to address this problem in the future by using boundary conditions derived from the

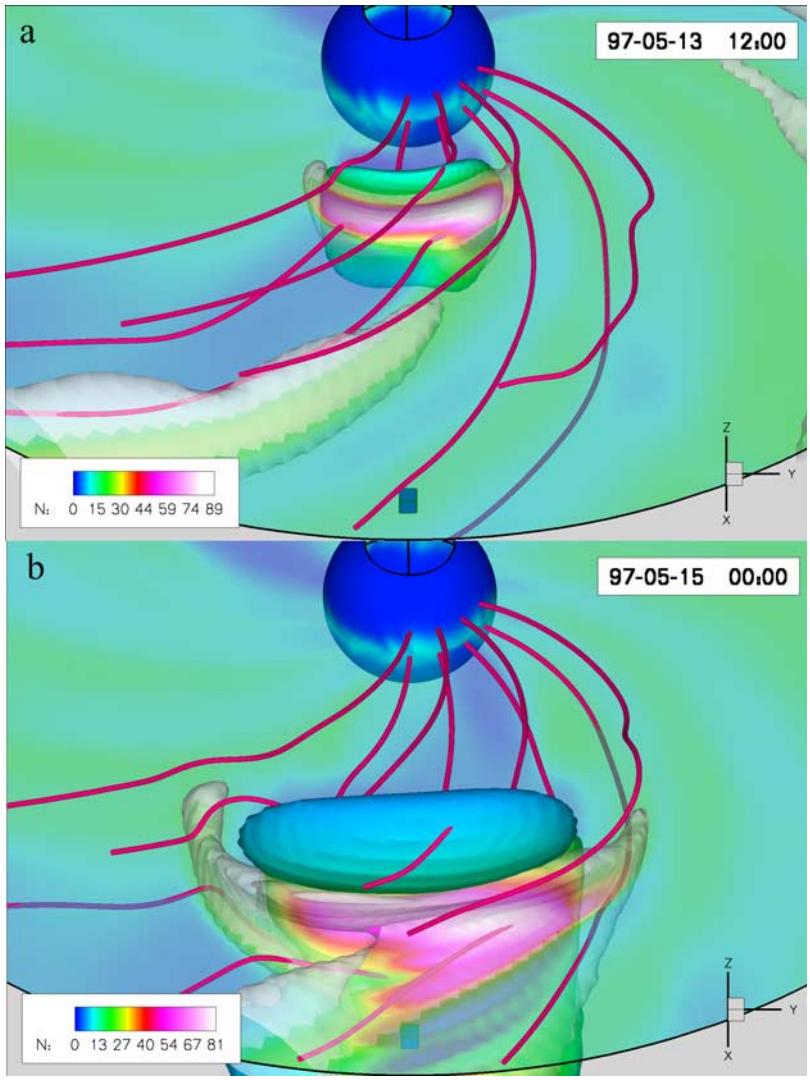

Figure 4. Visualization of disturbed solar wind parameters on May 13 12:00 UT (top panel) and May 15 00:00 UT (bottom panel). The number density is shown on the source surface and on the equatorial plane using the color scale (the coloring on the equatorial plane is translucent). The injected cloud is shown as an iso-surface at 25% of maximum value of its density (scaled by $(R_{AU}/r)^2$); the iso-surface is colored according to the corresponding value of the solar wind density. Magnetic field lines are shown as red lines. The Earth position is shown by a blue box.

SAIC and WSA models with higher-resolution, daily-updated boundary values.

6. Conclusion

[21] The work presented here is an attempt to demonstrate current capabilities and limitations of the 3-D MHD simulation when applied to a well-defined interplanetary event. We have used a relatively simple model based on photospheric observations of the solar magnetic field and coronagraph observations of the halo CME. Our predictions of the shock and ICME traveling times are expected to be slightly more accurate than the empirically derived relations [e.g., *Gopalswamy at al.*, 2001; *Schwenn et al.*, 2001] due to more realistic ambient solar wind and the use of observationally based inputs for the geometrical and kinematic properties of the CME. The main advantage of numerical simulations is in providing a global heliospheric picture, especially in cases when the CME interacts with solar wind stream structures. The present study suggests that high-quality solar observations can be used to predict the basic features of subsequent interplanetary disturbances.

[22] Knowledge of the prevailing ambient solar wind structure is essential for an understanding of the context of CME propagation as well as for predictions of recurrent geomagnetic storms. We have found that while large-scale recurrent stream structure can be predicted using available source surface maps, more effort is needed to match with observations throughout the solar activity cycle. In future, we plan to take advantage of ongoing improvements in the source surface model [*Arge and Pizzo*, 2000; *Arge at al.*, 2003] and the 3-D MHD coronal model with a more realistic thermodynamic treatment [*Lionello et al.*, 2001].

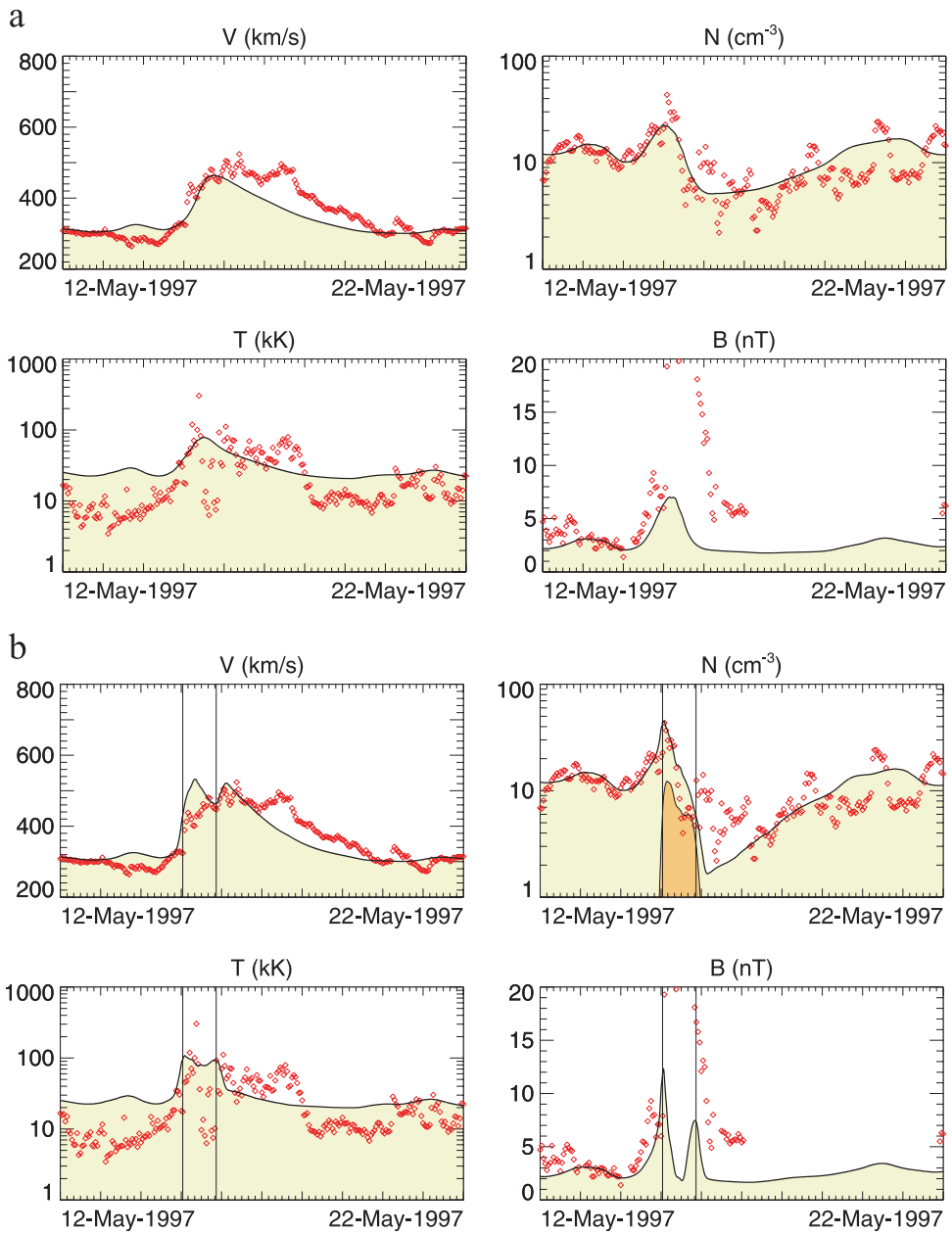

Figure 5. Evolution of solar wind parameters at Earth during the 12 May 1997 event. The top (bottom) panels show the flow velocity, number density, temperature, and magnetic field strength without (with) injection of the CME. Observed values are shown by red dots and results of the numerical simulation are shown by black solid lines. The superimposed observational data were obtained from the NASA's National Space Science Data Center (http://nssdc.gsfc.nasa.gov/cohoweb/cw.html). Vertical lines in the bottom panels indicate boundaries of the CME material indicated also by darker shading in the number density plot.

[23] Specification of transient disturbances is even more challenging. The hydrodynamic plasma cloud model used in this work may roughly simulate enhanced density structures seen in coronagraphs. Uncertainty in identifying the outer edges of rather fuzzy rings of halo CMEs and ignorance of eventual expansion and asymmetry of the CMEs causes errors in determining the free parameters of the cone model (and thus the diameter, location, and speed). Determination of the geometrical and kinematic properties of CMEs will be significantly improved by future Stereo observations providing angular perspectives away from the Sun-Earth line.

[24] Specification of the magnetic field structure remains a problem. While some 3-D analytic structures can be incorporated into a transient disturbance (as has been successfully done for basic investigations [e.g., *Detman et al.*, 1991; *Vandas et al.*, 2002; *Manchester et al.*, 2002]), this approach is ad hoc and will result in yet more free parameters. More accurate heliospheric simulations can be achieved by incorporating results from the numerical mod-

eling of the CMEs origin. Ultimately, we plan to drive the inner boundary of the heliospheric solution directly with output from the time-dependent coronal solution (see the first results given by *Odstrcil et al.* [2002]).

[25] As an interim solution, our specification of the ambient (based on the magnetic field topology of the coronal solution driven by photospheric magnetic field observations) and transient disturbances (based on geometrical and kinematic properties of halo CME coronagraph observations), appears to yield promising results. This model enables us to predict with improved fidelity the arrival of shocks and ICMEs, shock strength, solar wind parameters, and even magnetic field strength and orientation of the magnetic field in the sheath region between the shock and ejected plasma cloud. Simulation of magnetic cloud structures and prediction of the southward magnetic field component will require more modeling effort and the availability of new data, especially stereographic and heliospheric observations.

[26] **Acknowledgments.** This work has been supported by the DoD-AFOSR/MURI (Multi-Disciplinary Research Initiative), NSF/CISM (Center for Integrated Space Weather Modeling), and NASA/LWS (Living With a Star) projects. Additional support was from NASA Sun-Earth Connection Theory and Supporting Research and Technology Programs and by grants A3003003 and S10030067 from the Academy of Sciences and Grant Agency of the Czech Republic. Computational facilities were provided by National Center for Atmospheric Research in Boulder, CO. We acknowledge data from NSO Kitt Peak, ESA-NASA SOHO/LASCO project, and the NASA's National Space Science Data Center. We thank Vic Pizzo for useful discussions and reviewing the manuscript.

[27] Shadia Rifai Habbal thanks Ward Beecher Manchester IV and another referee for their assistance in evaluating this paper.

References

Arge, C. N., and V. J. Pizzo (2000), Improvement in the prediction of solar wind conditions using near-real time solar magnetic field updates, *J. Geophys. Res.*, *105*, 10,465–10,480.

Arge, C. N., D. Odstrcil, V. J. Pizzo, and L. Mayer (2003), Improved method for specifying solar wind speed near the Sun, in *Solar Wind Ten*, edited by M. Velli, R. Bruno, and F. Malara, *AIP Conf. Proc.*, *679*, 190–193.

Cane, H. V., and I. G. Richardson (2003), Interplanetary coronal mass ejections in the near-Earth solar wind during 1996–2002, *J. Geophys. Res.*, *108*(A4), 1156, doi:10.1029/2002JA009817.

Detman, T. R., M. Dryer, T. Yeh, S. M. Han, S. T. Wu, and D. J. McComas (1991), A time-dependent, three-dimensional MHD numerical study of interplanetary magnetic draping around plasmoids in the solar wind, *J. Geophys. Res.*, *96*, 9531–9540.

Dryer, M., C. D. Fry, W. Sun, C. S. Deehr, Z. Smith, S.-I. Akasofu, and M. D. Andrews (2001), Prediction in real-time of the 2000 July 14 heliospheric shock wave and its companions during the "Bastille" epoch, *Sol. Phys.*, *204*, 267–286.

Fry, C. D., M. Dryer, Z. Smith, W. Sun, C. S. Deehr, and S.-I. Akasofu (2003), Forecasting solar wind structures and shock arrival times using an ensemble of models, *J. Geophys. Res.*, *108*(A2), 1070, doi:10.1029/2002JA009474.

Gopalswamy, N., A. Lara, S. Yashiro, M. L. Kaiser, and R. A. Howard (2001), Predicting the 1-AU arrival times of coronal mass ejections, *J. Geophys. Res.*, *106*, 29,207–29,217.

Groth, C. P. T., D. L. DeZeeuw, T. I. Gombosi, and K. G. Powell (2000), Global three-dimensional MHD simulation of a space weather event: CME formation, interplanetary propagation, and interaction with the magnetosphere, *J. Geophys. Res.*, *105*, 25,053–25,078.

Hundhausen, A. J. (1993), Size and locations of coronal mass ejections: SMM observations from 1980 and 1984–1989, *J. Geophys. Res.*, *98*, 13,177–13,200.

Linker, J., Z. Mikic, D. A. Biesecker, R. J. Forsyth, W. E. Gibson, A. J. Lazarus, A. Lecinski, P. Riley, A. Szabo, and B. J. Thompson (1999), Magnetohydrodynamic modeling of the solar corona during whole sun month, *J. Geophys. Res.*, *104*, 9809–9830.

Lionello, R., J. A. Linker, and Z. Mikic (2001), Including the transition region in models of the large-scale solar corona, *Astrophys. J.*, *546*, 542–551.

Manchester, W. B., I. Roussev, M. Opher, T. Gombosi, D. DeZeeuw, G. Toth, I. Sokolov, and K. Powell (2002), 3D MHD simulation of CME propagation from solar corona to 1 AU, *Eos Trans. AGU*, *83*(47), Fall Meet. Suppl., abstract SH21A-0501.

Odstrcil, D., and V. J. Pizzo (1999a), Three-dimensional propagation of coronal mass ejections (CMEs) in a structured solar wind flow: 1. CME launched within the streamer belt, *J. Geophys. Res.*, *104*, 483–492.

Odstrcil, D., and V. J. Pizzo (1999b), Distortion of interplanetary magnetic field by three-dimensional propagation of CMEs in a structured solar wind, *J. Geophys. Res.*, *104*, 28,225–28,239.

Odstrcil, D., M. Dryer, and Z. Smith (1998), Numerical simulation of March 1991 interplanetary disturbances (SOLTIP Interval I), in *Proceedings of the Third SOLTIP Symposium*, edited by X. S. Feng, F. S. Wei, and M. Dryer, pp. 191–199, Int. Acad., Beijing.

Odstrcil, D., J. A. Linker, R. Lionello, Z. Mikic, P. Riley, V. J. Pizzo, and J. G. Luhmann (2002), Merging of coronal and heliospheric numerical two-dimensional MHD models, *J. Geophys. Res.*, *107*(A12), 1493, doi:10.1029/2002JA009334.

Plunkett, S. P., et al. (1997), The relationship of green-line transients to white-light coronal mass ejections, *Sol. Phys.*, *175*, 699.

Plunkett, S. P., B. J. Thompson, R. A. Howard, D. J. Michels, O. C. St. Cyr, S. J. Tappin, R. Schwenn, and P. L. Lamy (1998), LASCO observations of an Earth-directed coronal mass ejection on May 12, 1997, *Geophys. Res. Lett.*, *25*, 2477.

Riley, P., J. A. Linker, and Z. Mikic (2001), An empirically driven global MHD model of the solar corona and inner heliosphere, *J. Geophys. Res.*, *106*, 15,889–15,901.

Schmidt, J. M., and P. J. Cargill (2001), Magnetic cloud evolution in a two-speed solar wind, *J. Geophys. Res.*, *106*, 8283–8289.

Schwenn, R., A. Dal Lago, W. D. Gonzales, E. Huttunen, C. O. St. Cyr, and S. P. Plunkett (2001), A tool for improved space weather predictions: The CME expansion speed, *Eos Trans. AGU*, *82*(47), Fall Meet. Suppl., abstract SH12A-0739.

Toth, G., and D. Odstrcil (1996), Comparison of some flux corrected transport and total variation diminishing numerical schemes for hydrodynamic and magnetohydrodynamic problems, *J. Comput. Phys.*, *128*, 82–100.

Usmanov, A. V. (1993), A global numerical 3-D MHD model of the solar wind, *Sol. Phys.*, *145*, 377–396.

Vandas, M., D. Odstril, and S. Watari (2002), Three-dimensional MHD simulation of a loop-like magnetic cloud in the solar wind, *J. Geophys. Res.*, *107*(A9), 1236, doi:10.1029/2001JA005068.

Webb, D. F., et al. (1997), Large-scale structures and multiple neutral lines associated with coronal mass ejections, *J. Geophys. Res.*, *102*, 24,161.

Webb, D. F., R. P. Lepping, L. F. Burlaga, C. E. DeForest, D. E. Larson, S. F. Martin, S. P. Plunkett, and D. M. Rust (2000), The origin and development of the May 1997 magnetic clouds, *J. Geophys. Res.*, *105*, 27,251–27,259.

Wu, C.-C., M. Dryer, and S. T. Wu (1996), Three-dimensional MHD simulation of interplanetary magnetic field changes at 1 AU as a consequences of simulated solar flares, *Ann. Geophys.*, *14*, 383–399.

Zhao, X. P., and D. F. Webb (2003), Source regions and storm effectiveness of frontside full halo coronal mass ejections, *J. Geophys. Res.*, *108*(A6), 1234, doi:10.1029/2002JA009606.

Zhao, X. P., S. P. Plunkett, and W. Liu (2002), Determination of geometrical and kinematical properties of halo coronal mass ejections using the cone model, *J. Geophys. Res.*, *107*(A8), 1223, doi:10.1029/2001JA009143.

D. Odstrcil, NOAA, Space Environment Center, 325 Broadway, Boulder, CO 80305, USA. (dusan.odstrcil@noaa.gov)

P. Riley, Science Applications International Corporation, 10260 Campus Point Drive, San Diego, CA 92121, USA. (pete.riley@saic.com)

X. Zhao, W. W. Hansen Experimental Physics Laboratory, Stanford University, Stanford, CA 94305, USA. (xpzhao@solar.stanford.edu)